

# CR DEL - LONG TERM INVESTIGATION OF PERIOD BEHAVIOUR

BERTHOLD, THOMAS<sup>1,2</sup>; HÄUSSLER, KLAUS<sup>1,2</sup>; HUNGER, DIETER<sup>1</sup>; JACOBS, BJÖRN<sup>1</sup> AND STEINGRÜBER, JAN<sup>1</sup>

1) Sternwarte Hartha, Töpelstr. 49, 04746 Hartha, Germany, [info@sternwarte-hartha.de](mailto:info@sternwarte-hartha.de)

2) BAV - Bundesdeutsche Arbeitsgemeinschaft für Veränderliche Sterne, Munsterdamm 90, 12169 Berlin, Germany

**Abstract:** Almost 80 years of photometric history of this RRc type variable star are presented. The period has found to be stable with a likely trend to increase typical for that type of stars.

## 1 Introduction

CR Del (GSC 01632–01154, UCAC4 529–132455) has been discovered to be variable by Ahnert et. al (1947) and reported to be of EB type by Kreiner (2004). More recent surveys (ASAS, ASAS-SN, Zwicky Transient Facility and GAIA DR2) revealed the RRc pulsating nature of CR Del. In order to improve the precision and check the validity of these results over some decades photographic plates from the Sonneberg Observatory Astrographs, exposed from 1942 to 1994 were used. Contemporary complementation was done by photoelectric photometry.

## 2 Observations

The photographic plate archive of the Sonneberg Observatory offers unique possibilities for long term studies of variable stars. A total of 216 digital scans from blue sensitive plates of the Sonneberg astrographs (400mm/f4 and 400mm/f4.75, limiting magnitude 16.5 mag<sub>phot</sub>) has been used for visual brightness estimations done by DH, BJ and JS. The exposure time of these plates varied from 30 to 60 minutes according to sky quality.

Table 1: Photographic comparison stars. Blue band magnitudes for use with photographic plates according to Zacharias N., Finch C.T., Girard T.M. et al. (2013).

Star	ID	RA [h:m:s]	DEC [° ' "]	<i>B</i> [mag]
a	UCAC4 528–136699	20 28 51.9	+15 33 19.2	13.532
b	UCAC4 529–132430	20 28 46.4	+15 38 29.0	14.039
c	UCAC4 529–132475	20 28 53.5	+15 39 22.9	14.636
d	UCAC4 529–132463	20 28 51.6	+15 36 07.0	15.148

One of the authors (TB) has performed photometry to ensure the validity of the results from the plate studies. The Hartha Observatory 36cm f14.5 Cassegrain telescope was used attached with a Canon EOS 1100D camera without filter. Bayer array G-Band intensities

Table 2: Photometric comparison stars.  $V$  band magnitudes for use with CMOS  $G$ -Band. Both stars were used in ensemble mode. Magnitudes according to Zacharias N., Finch C.T., Girard T.M. et al. (2013).

Star	ID	RA [h:m:s]	DEC [° ' "]	$V$ [mag]
Comp1	UCAC4 529–132497	20:28:58.6	+15:37:08.8	13.215
Comp2	UCAC4 529–132430	20:28:46.4	+15:38:29.0	12.953

( $n = 281$ ) were read from the CMOS Sensor to provide data nearly the Johnson  $V$ -Band. Exposure time was 90 seconds at ISO 1600.

Individual frames have been dark and flat field corrected and differential aperture photometry was applied for the data analysis using the C-Munipack v2.1 software package (Motl, 2021). RMS of the differential brightness (Var-Comp) was 0.018 mag.

## 2.1 Light curves

Figures 1 and 2 give the folded light curves of the two observational data sets. The larger scatter for the historic observations is due to the method of visual estimating the brightnesses as well as the long exposure times of the plates. Apart from this the shape of the light curves is comparable.

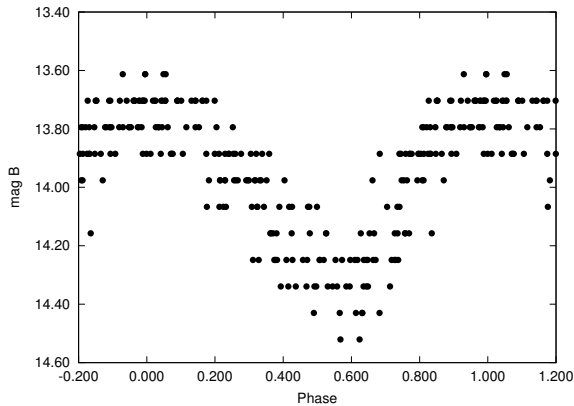


Figure 1: Phase diagram of visual estimates from the Sonneberg plates folded on ephemeris (2). Magnitudes refer to the  $B$  magnitudes from Tab. 1

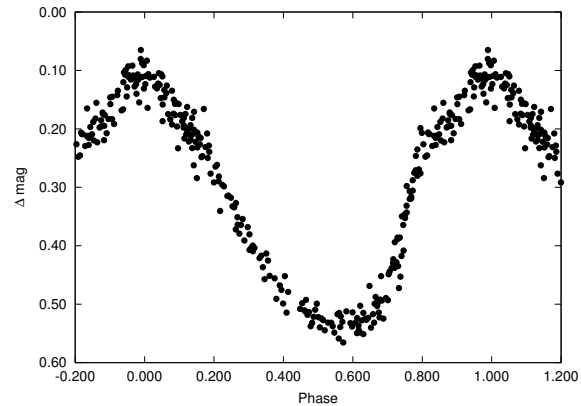


Figure 2: Photometric phase diagram folded on ephemeris (2). Magnitudes refer to 13.084 mag  $V$  due to ensemble mode photometry using comparison stars from Tab. 2

## 2.2 Times of maximum light

Times of maxima from the photographic observations were derived as normal maxima from polynomial fitted sub-light curves for time intervals of 3-5 years well filled with observations. Applying such an approach carefully avoids cycle count errors which otherwise is a serious threat in the analysis of O–C diagrams from long time series with gaps.

Furthermore other available surveys were searched using the Photometric Data Retriever (PDR) software from Zejda et al. (2019) to obtain additional data.

Data from the surveys as well as the photometric measurements were also derived from polynomial fits of the corresponding light curves.

Table 3 gives the overview for these data together with their individual errors and sources. The values given there have been used for this long term period study.

Table 3: Times of maximum light. The two sets of O–C values are computed with respect to the linear and quadratic fit respective (see section 2.3).

HJD	Error	Epoch	O–C(1)	O–C(2)	Source
2430606.388	0.013	–112579	+0.014	–0.004	Photographic
2438287.404	0.008	–82634	–0.001	+0.004	Photographic
2439388.308	0.017	–78342	–0.014	–0.007	Photographic
2444116.467	0.022	–59909	–0.005	+0.008	Photographic
2448504.223	0.018	–42803	–0.017	–0.003	Photographic
2453913.404	0.034	–21715	–0.006	+0.003	ASAS3 Grade A
2457186.148	0.010	–8956	–0.004	–0.001	GAIA DR2
2457316.7071	0.0058	–8447	–0.0059	–0.0034	ASAS–SN V
2458763.6561	0.0094	–2806	+0.0004	–0.0006	ASAS–SN g
2458829.5767	0.0054	–2549	–0.0006	–0.0018	ZTF–g
2459472.3864	0.0069	–43	+0.0085	+0.0055	Photometric
2459483.4123	0.0069	0	+0.0047	+0.0017	Photometric

### 2.3 Ephemeris and O–C diagramm

First a  $(1/\text{Error}^2)$ -weighted linear least squares fit of the times of maximum light from Table 3 yields

$$HJD_{\text{Max}} = 2459483.4076(23) + 0.25650462(6) \cdot E. \quad (1)$$

The results shown in Figure 3 suggest to try a parabolic fit.

$$HJD_{\text{Max}} = 2459483.4106(15) + 0.25650535(16) \cdot E + 76(17) \cdot 10^{-13} \cdot E^2 \quad (2)$$

The standard deviation of the residuals decreases from 0.0088 to 0.0045 days when the parabolic ephemerides are used. From the statistic point this gives some trust to the quadratic solution.

## 3 Results

The quadratic term in ephemerides (2) can be used to obtain a value for the rate of the period increase.

$$\dot{P} = dP/dt = 5.93(1.31) \cdot 10^{-11} \text{ day/day} = 0.022(5) \text{ day/Ma} \quad (3)$$

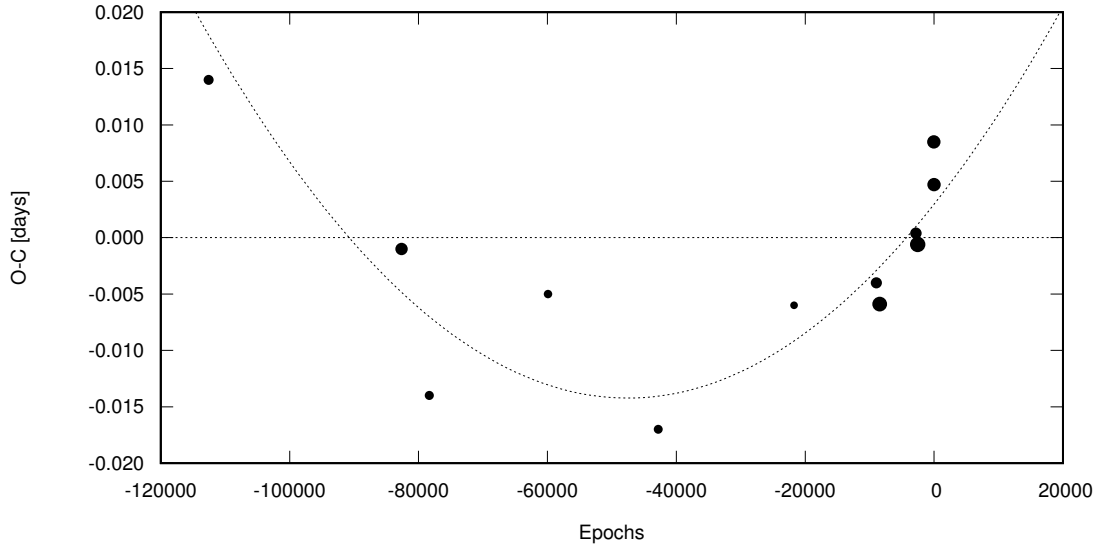


Figure 3: O–C diagram of CR Del. Size of symbols refers to the individual weights derived from their errors. The dashed line and parabola correspond to ephemeris (1) or (2) respective.

Such a constant increase is small enough for a helium burning horizontal branch star (Neilson, Percy&Smith (2016) with further sources therein). This amount is also in good agreement to the size of values obtained for other RRc type stars in the paper of Percy&Tan (2013).

Although the remaining scatter of the timings is considerable the lesser amount of residuals leads us to the assumption of a valid parabolic solution. At worst the above value yields an upper limit to the rate of period change at least.

## 4 Summary

Deriving rates of period changes in RRc stars is difficult because of their sinusoidal shape of light curves. To overcome this the use of data out of a long period of time can be a useful way. Small amounts of period changes can accumulate over decades to reach well determinable shifts in the position of maximum light.

CR Del shows a constantly increasing period over the investigated time interval what can be expected according to the predictions of stellar evolution models.

**Acknowledgements:** The authors are pleased to acknowledge the use of plate scans from Sonneberg Observatory Plate Archive. This research has made use of the SIMBAD database and the VizieR catalogue access tool, operated at CDS, Strasbourg, France (Wenger et al. 2000). Data from ASAS All Star Catalogue (asas3, Pojmanski, 1997), ASAS-SN All-Sky Automated Survey (Shappee et al., 2014; and Kochanek et al., 2017) as well as the Zwicky Transient Facility (DR7), maintained by the NASA/IPAC Infrared Science Archive, which is funded by the National Aeronautics and Space Administration and operated by the California Institute of Technology. This work has made use of data from the European Space Agency (ESA) mission *Gaia* (<https://www.cosmos.esa.int/gaia>), processed

by the *Gaia Data Processing and Analysis Consortium (DPAC)*  
(<https://www.cosmos.esa.int/web/gaia/dpac/consortium>).

## References

- Ahnert, P., Hoffmeister, C., Rohlfs, E. et al. 1947, *Veroeff. Sternwarte Sonneberg*, **1**, 43, [1947VeSon...1...43A](#)
- Kochanek, C. S. et al. 2017, *Publications of the Astronomical Society of the Pacific*, **129**, 980, [2017PASP..129j4502K](#)
- Gaia Collaboration et al. 2016, *A&A*, **595**, A1, [2016A&A...595A...1G](#)
- Gaia Collaboration et al. 2018, *A&A*, **616**, A1, [2018A&A...616A...1G](#)
- Kreiner, J. M. 2004, *Acta Astron.*, **54**, 207, [2004AcA....54..207K](#)
- Motl, D., 2021, C-Munipack 2.1, <https://sourceforge.net/projects/c-munipack/files/>
- Neilson, H.R., Percy, J.R. & Smith, H.A. 2016, *J. Amer. Assoc. Var. Star Obs.*, **44**, 179, [2016JAVSO..44..179N](#)
- Percy, J.R. & Tan, P.J. 2013, *J. Amer. Assoc. Var. Star Obs.*, **41**, 1, [2013JAVSO..41...75P](#)
- Pojmanski, G. 1997, *Acta Astron.*, **47**, 467, [1997AcA....47..467P](#)
- Shappee, B. J. et al. 2014, *The Astrophysical Journal*, **788**, 48, [2014ApJ...788...48S](#)
- Wenger, M. et al. 2000, *Astronomy and Astrophysics Supplement*, **143**, 9, [2000A&AS..143....9W](#)
- Zacharias N., Finch C.T., Girard T.M. et al 2013, *AJ*, **145**, 44, [2013AJ....145...44Z](#)
- Zejda, M., Skýba, O., Krajčovič, M. et al. 2019, *Contr. Astron. Obs. Skalnaté Pleso*, **49**, 132, [2019CoSka..49..132Z](#)